

Photofragment Spectroscopy of FeCH_2^+ , CoCH_2^+ , and NiCH_2^+ near the M^+-CH_2 Dissociation Threshold

John Husband, Fernando Aguirre, Christopher J. Thompson, Christopher M. Laperle, and Ricardo B. Metz*

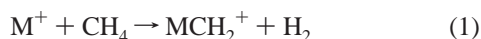
Department of Chemistry, University of Massachusetts, Amherst, Massachusetts 01003

Received: October 12, 1999; In Final Form: December 24, 1999

Photofragment spectra of jet-cooled MCH_2^+ ($\text{M} = \text{Fe}, \text{Co}, \text{Ni}$) have been measured. Our investigation of NiCH_2^+ represents the first reported spectroscopic study of this molecule. A spectroscopic threshold is observed for each of the three systems. In addition to imposing strict *upper limits* on the M^+-CH_2 bond strengths, these results further the discussion concerning the interpretation of spectroscopic thresholds as thermodynamic limits. The measured upper limits are: $D^{\circ}_0(\text{Fe}^+-\text{CH}_2) \leq 342 \pm 2$ kJ/mol, $D^{\circ}_0(\text{Co}^+-\text{CH}_2) \leq 331 \pm 2$ kJ/mol, and $D^{\circ}_0(\text{Ni}^+-\text{CH}_2) \leq 295 \pm 5$ kJ/mol. Three distinct, 2-nm-wide peaks are observed in the photofragment spectrum of CoCH_2^+ , but the spectra lack sharp structure above threshold.

Introduction

Transition metals are essential components of diverse reaction systems. Nature's catalyst of choice at the enzyme level, transition metal based catalysts have also been prevalent in industry since the first plant for the oxidation of SO_2 to SO_3 over platinum went on line in 1875.¹ The group VIII metals have from the beginning been by far the most utilized. However, despite their many successful applications, the large-scale, efficient activation of methane has proven to be an elusive goal for traditional catalysis. To this end, recent attention² has focused on gas-phase transition metal cations, M^+ . While reactions of first-row M^+ with methane are endothermic,² the third-row group VIII metals, $\text{M} = \text{Os}, \text{Ir},$ and Pt , in addition to $\text{M} = \text{Ta}$ and W , will spontaneously dehydrogenate methane.³ Often, sequential reactions exhibiting Fischer-Tropsch type methylene coupling occur:



Irikura and Beauchamp³ have reported oligomerizations forming compounds as large as $\text{WC}_8\text{H}_{16}^+$. Such oligomerizations have a direct analogy with surface chemistry where incorporation of hydrocarbons into the $\text{M}-\text{CH}_2$ bond of CH_2 moieties chemisorbed onto metal surfaces is a crucial chain growth step in the Fischer-Tropsch process.⁴ Studies of isolated, gas-phase MCH_2^+ offer the opportunity to understand the intrinsic properties of these systems. As part of an ongoing effort to characterize the intermediates involved in the activation of methane by transition metal cations, we report the photodissociation spectra of MCH_2^+ ($\text{M} = \text{Fe}, \text{Co},$ and Ni).

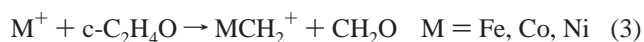
MCH_2^+ systems have had a rich history over the last two decades. Results of experimental and theoretical investigations for $\text{M} = \text{Fe}, \text{Co},$ and Ni will be summarized as each system is discussed in turn. A thorough review of the reactions of M^+ has been given by Eller and Schwarz.²

Experimental Section

The experimental setup has been described in detail elsewhere.⁵ Briefly, ions produced in the source are mass selected

and photodissociated at the turning point of a reflectron, and the masses of fragment ions are determined by time-of-flight.

Metal ions are produced by laser ablation of a rotating and translating rod (Fe , Sigma-Aldrich, 99.98% pure; Co , Sigma-Aldrich, 99.95% pure; Ni , Strem, 99+% pure). The resulting plasma is entrained in a pulse of bath gas, seeded with a small amount of ethylene oxide ($\text{c-C}_2\text{H}_4\text{O}$, Merriam-Graves, 99.7% pure). MCH_2^+ is formed by reaction 3 and cools via collisions



with the bath. While reaction 3 is exothermic and efficient for Fe and Co , it is ~ 17 kJ/mol endothermic for Ni and highly inefficient. The parent ion mass spectrum for $\text{Ni}^+ + \text{c-C}_2\text{H}_4\text{O}$ is dominated by $\text{Ni}^+\cdot\text{c-C}_2\text{H}_4\text{O}$ and heavier adducts, with the NiCH_2^+ signal 1 order of magnitude smaller than that for FeCH_2^+ or CoCH_2^+ . The relatively small amounts of NiCH_2^+ formed likely originate from the reaction of internally or translationally excited Ni^+ . Since NiCH_2^+ formed in this manner undergoes many cooling collisions before expansion into the source chamber, it is internally cold at the point of investigation despite its hot origins. The choice of bath gas varies slightly for each system. A mixture of 3% $\text{c-C}_2\text{H}_4\text{O}$, 5% N_2 in He at a backing pressure of 4 atm effectively cools FeCH_2^+ . The presence of N_2 in the gas mixture raises the possibility of forming FeN^+ which has the same nominal mass as FeCH_2^+ . Comparison of spectra obtained with and without N_2 show that the presence of N_2 has no effect on the intensity of the 70 amu mass peak, and its sole effect on the photofragment spectra is to more clearly define the assigned threshold. Therefore the spectrum reported is due to FeCH_2^+ and not FeN^+ . For CoCH_2^+ it is necessary to substitute O_2 for N_2 thereby increasing the efficiency with which excited electronic states are quenched; best results are obtained with 1% $\text{c-C}_2\text{H}_4\text{O}$, 5% O_2 in He . Backing pressures as high as 7 atm have been used, but no additional cooling is observed beyond 4 atm. A similar mixture, 2% $\text{c-C}_2\text{H}_4\text{O}$, 5% O_2 in He , at 4 atm is used for the NiCH_2^+ study. This source, operating under similar conditions, has been shown⁵ to produce electronically and vibrationally cold ions with rotational temperatures of ~ 10 K.

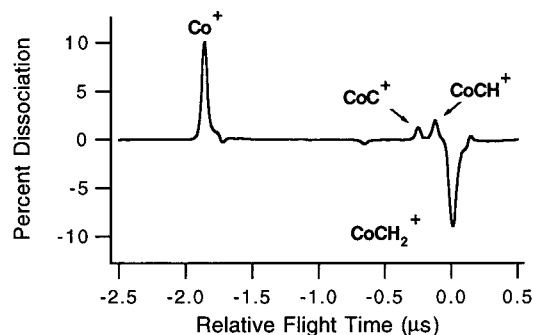


Figure 1. Photodissociation of CoCH_2^+ at 320 nm. Three clearly resolvable channels, leading to loss of H, H_2 , and CH_2 , are active at this wavelength.

As all species exit the mixing area they expand supersonically into vacuum, are skimmed into a differentially pumped chamber, and enter the extraction region of a Wiley–McLaren time-of-flight mass spectrometer.⁶ Positive ions accelerate to 1800 V kinetic energy and pass into a field-free flight tube. The frequency-doubled output of a Nd:YAG-pumped tunable dye laser photodissociates the ions at the turning point of a reflectron. Wavelengths greater than 364 nm are produced by mixing the output of the dye laser with the 1064 nm Nd:YAG fundamental. Line widths are $\sim 0.2 \text{ cm}^{-1}$ at wavelengths below 364 nm and $\sim 1 \text{ cm}^{-1}$ above.

Parent and photofragment ions reaccelerate out of the reflectron, traverse a field-free region, and impinge upon a 40-mm-diameter dual microchannel plate detector. Masses are determined from their characteristic flight times. There is a 5° angle between the flight paths of ions in to and out of the reflectron. Pulsing the deflector plate voltage necessary to create this angle forms an effective mass gate as only those ions within the deflector at the time of the pulse follow a path through the reflectron terminating at the detector.

Subtracting spectra collected with the dissociation laser blocked from those when it is unblocked produces a difference spectra as shown in Figure 1. This allows immediate identification of the dissociation channels active at a given wavelength, as well as giving the relative importance of each. The area under the M^+ fragment is integrated, normalized to the MCH_2^+ parent intensity and dissociation laser fluence, and plotted against the dissociation laser wavelength to produce a photofragment spectrum.

For each of the systems reported here, in addition to loss of CH_2 , loss of a H atom and H_2 is energetically allowed⁷ in portions of the spectral region covered. Indeed a previous low-resolution study by Hettich and Freiser⁷ shows the spectroscopic threshold for loss of H_2 to occur below that for CH_2 loss. However, while all three channels are observed, it is loss of CH_2 which constitutes the major dissociation channel and is the focus this paper.

Results

Photofragment spectra near the threshold for M^+-CH_2 bond dissociation are shown in Figures 2–4. In each case the spectra are those of MCH_2^+ containing the major metal isotope only: $\text{M} = {}^{56}\text{Fe}$, 92%; $\text{M} = {}^{59}\text{Co}$, 100%; $\text{M} = {}^{58}\text{Ni}$, 68%. These spectra were recorded using an unfocused laser beam and low laser fluence to minimize contributions from two-photon processes. Fluences were kept within a range of 14–28 mJ/cm^2 , typically $\sim 18 \text{ mJ}/\text{cm}^2$. Dissociation is linear with respect to fluences up to at least 35 mJ/cm^2 .

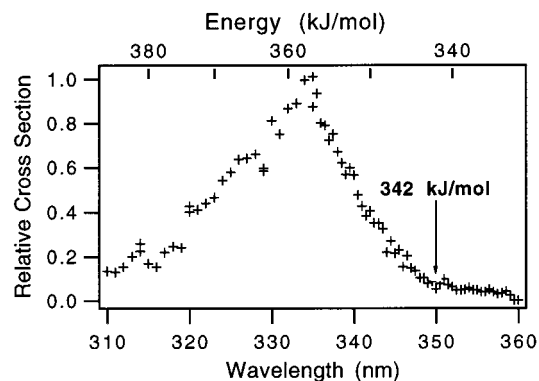


Figure 2. Photofragment spectrum of $\text{FeCH}_2^+ + h\nu \rightarrow \text{Fe}^+ + \text{CH}_2$. The Fe^+ photosignal has been normalized to the parent ion intensity and laser power. A relative cross section of 1 corresponds to approximately $4 \times 10^{-18} \text{ cm}^2$.

Before discussion of the three systems individually, some general observations may be made. In each case at threshold energy there is a distinct increase in the M^+ photosignal. Above the threshold energy, dissociation cross sections as high as $\sim 4 \times 10^{-18} \text{ cm}^2$ are observed. Below the threshold energy only extremely low levels of nonresonant background signal are found. Three distinct, 2-nm-wide peaks are observed in the photofragment spectrum of CoCH_2^+ , but the spectra lack sharp structure above threshold.

FeCH_2^+ . The photofragment spectrum for internally cold FeCH_2^+ from 310 to 360 nm is shown in Figure 2. The Fe^+ photosignal rises steadily from 315 nm to a maximum at 335 nm before dropping off to baseline at 350 nm. In 1986, Hettich and Freiser⁷ obtained the photofragment spectrum of FeCH_2^+ in a ICR cell using a lamp–monochromator combination with 10 nm resolution. The 310–360 nm section closely resembles our results, the only significant difference being their observation of a tail extending from 350 nm to longer wavelengths. The authors attributed the tail to the photodissociation of hot ions and assigned a cutoff at 350 nm, establishing the *upper limit* $D^0(\text{Fe}^+-\text{CH}_2) \leq 342 \pm 20 \text{ kJ/mol}$. Our results, in complete agreement, show the spectroscopic threshold for dissociation of internally cold FeCH_2^+ occurs at 350 nm and that, even at the much higher resolution of this study, the spectrum is unstructured. Photodissociation of internally cold ions and improved resolution allow us to refine the *upper limit* to $D^0_0(\text{Fe}^+-\text{CH}_2) \leq 342 \pm 2 \text{ kJ/mol}$. In a complementary ion-beam experiment, Schultz and Armentrout measured the Fe^+-CH_2 bond strength on the basis of the formation of FeCH_2^+ in the endothermic $\text{Fe}^+ + \text{c-C}_3\text{H}_6$ reaction.⁸ They also measured the Fe^+-CH_2 bond strength on the basis of the threshold for forming FeCH_2^+ from collision-induced dissociation of Fe^+ -cyclopropane:



This second measurement allowed a straightforward calculation of $D^0_0(\text{Fe}^+-\text{CH}_2)$ which matched the first precisely. Armentrout has recently reevaluated these results to give a value of $D^0_0(\text{Fe}^+-\text{CH}_2) = 341 \pm 4 \text{ kJ/mol}$.⁹

The first-row group VIII MCH_2^+ systems have been the subject of numerous theoretical investigations.^{10–24} Calculations of the dissociation energies of these systems fall into two broad classes: those employing an ab initio approach and those using density functional methods. Among the most sophisticated of the ab initio calculations are those performed by Bauschlicher et al.^{13–15} and those of Morokuma and co-workers.^{16–19} Baus-

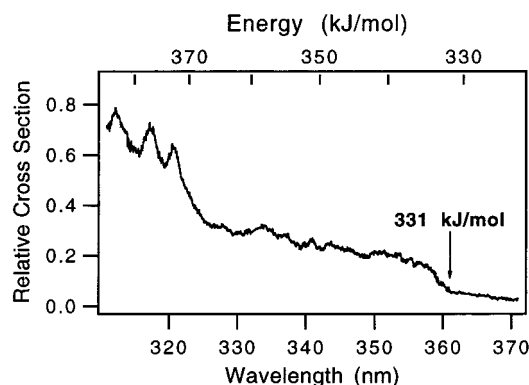


Figure 3. Photofragment spectrum of $\text{CoCH}_2^+ + h\nu \rightarrow \text{Co}^+ + \text{CH}_2$. The Co^+ photosignal is shown relative to that of Fe^+ from FeCH_2^+ , for which a value of 1 corresponds to approximately $4 \times 10^{-18} \text{ cm}^2$.

chlicher et al.¹⁵ using an ICACPF (internally contracted averaged coupled-pair functional) method gave a best estimate of $D^{\circ}_0(\text{Fe}^+-\text{CH}_2)(^4\text{B}_1) = 310 \text{ kJ/mol}$. Musaev and Morokuma¹⁹ predict $D^{\circ}_0(\text{Fe}^+-\text{CH}_2)(^4\text{B}_2) = 283 \text{ kJ/mol}$ at the MR-SDCI CASSCF(9/10) + Davidson correction level of theory. Holthausen et al.²¹ used a variety of parametrized density functional/Hartree-Fock hybrid methods in their calculations. For the late-first-row metals, experimental values were most closely matched using the B3LYP hybrid scheme, combined with an all-electron treatment of the metal. This approach yielded $D^{\circ}_0(\text{Fe}^+-\text{CH}_2)(^4\text{B}_1) = 348 \text{ kJ/mol}$. Dissociation energies in each case have been given relative to the ground state of FeCH_2^+ as predicted by the respective studies. These studies show the ground state to be one of a pair of nearly degenerate states. Bauschlicher et al.¹⁵ and Holthausen et al.²¹ predict a $^4\text{B}_1$ ground state, whereas Musaev and Morokuma¹⁹ predict the $^4\text{B}_2$ state to be the ground state. In addition a $^4\text{A}_2$ state lies $\sim 8 \text{ kJ/mol}$ above this pair.¹⁹

CoCH₂⁺. The photofragment spectrum of CoCH_2^+ is, of the three systems reported here, potentially the most rich in information. The spectrum, shown in Figure 3, consists of three $\sim 2\text{-nm}$ -wide peaks centered at 312.3, 317.3, and 320.5 nm followed by a drop to a plateau at 324 nm. Beyond this threshold the Co^+ photosignal remains constant as the wavelength increases until a second threshold is reached at 361 nm. Our results differ in several key aspects from the low-resolution photofragment spectrum previously obtained by Hettich and Freiser.⁷ At the lower resolution the three 2-nm-wide peaks and the threshold at 324 nm merge into a continuous feature extending from 290 to 340 nm. Above 340 nm the Co^+ photosignal slowly decreases, disappearing by 390 nm. Hettich and Freiser attributed the observed signal in the region from 340 to 390 nm to the dissociation of hot ions since this signal decreased with increasing pressure of Ar used to cool the parent ions. The threshold was thus assigned at 340 nm, giving $D^{\circ}_0(\text{Co}^+-\text{CH}_2) \leq 351 \pm 20 \text{ kJ/mol}$.⁷ This value agreed with an early ion beam value of $D^{\circ}_0(\text{Co}^+-\text{CH}_2) = 355 \pm 30 \text{ kJ/mol}$, measured by Armentrout and Beauchamp.²⁵ With the forewarning of the possibility of a large contribution from the dissociation of hot ions, care was taken to ensure our ions were cooled as fully as possible. While we do find photodissociation beyond 361 nm to be effectively eliminated as the ions are cooled, the threshold at 361 nm is observed regardless of source conditions. Indeed, cooling the ions serves only to improve the definition of the threshold. Thus, as a result of starting with internally cold ions and with the increased resolution of this study, we are able to reestablish $D^{\circ}_0(\text{Co}^+-\text{CH}_2) \leq 331 \pm 2 \text{ kJ/mol}$. Fisher and Armentrout, using a second-generation guided ion-beam spectrometer,²⁶ returned to the CoCH_2^+ system to measure the

thermodynamic Co^+-CH_2 bond strength. Armentrout has recently reevaluated⁹ these results to give $D^{\circ}_0(\text{Co}^+-\text{CH}_2) = 318 \pm 5 \text{ kJ/mol}$, which is consistent with our upper limit value. Bauschlicher et al.¹⁵ give a best estimate $D^{\circ}_0(\text{Co}^+-\text{CH}_2) = 331 \text{ kJ/mol}$ in agreement with Musaev et al.¹⁷ (336 kJ/mol); Holthausen et al.²¹ calculate $D^{\circ}_0(\text{Co}^+-\text{CH}_2) = 315 \text{ kJ/mol}$. All three studies predict the ground state of CoCH_2^+ to be the nearly degenerate $^3\text{A}_1$ and $^3\text{A}_2$ states. Bauschlicher et al.¹⁵ and Holthausen et al.²¹ calculate the $^3\text{A}_2$ state to be slightly lower in energy while Musaev et al.¹⁷ have this order reversed. Two more states, a $^3\text{B}_1$ and a $^3\text{B}_2$, are predicted to lie within 35 kJ/mol of the ground state.¹⁷

In addition to the threshold at 361 nm, we observe a second threshold at 324 nm, 38 kJ/mol above the first. The first electronically excited states of Co^+ ($^5\text{F}_0$) and CH_2 ($^1\text{A}_1$) occur at 40 and 38 kJ/mol, respectively.^{27,28} This suggests that this second threshold occurs once sufficient energy is available to access repulsive states of CoCH_2^+ arising from the ^5F or $^1\text{A}_1$ fragment states. This issue is expanded upon in the next section.

Three $\sim 2\text{-nm}$ -wide peaks are observed centered at 312.3, 317.3, and 320.5 nm, corresponding to spacings of 504 and 315 cm^{-1} . First-order spin-orbit splittings are not found in a molecule with nondegenerate electronic states,²⁹ and second-order splittings would not be expected to result in spacings this large. The peaks therefore most likely represent one or more vibrational progressions in an excited electronic state. Plausible candidates are the Co^+-CH_2 stretch (ν_3) and the CH_2 in-plane rock (ν_6). A transition from a Co^+-C bonding orbital to one of nonbonding or antibonding character would be expected to produce a progression in the Co^+-CH_2 stretch. Ricca and Bauschlicher²² have shown the ground states of ScCH_2^+ and TiCH_2^+ to be significantly distorted from C_{2v} symmetry along the CH_2 in-plane rock coordinate, suggesting the observed features could be due to a vibrational progression in ν_6 as a result of a similar distortion in the excited state of CoCH_2^+ . Vibrational constants for high-lying electronic states of CoCH_2^+ have yet to be calculated or measured. However, Ricca and Bauschlicher²² calculate $\omega_3 = 634 \text{ cm}^{-1}$ and $\omega_6 = 632 \text{ cm}^{-1}$ for the ground ($^3\text{A}_2$) state at the B3LYP level of theory. Musaev et al.¹⁷ give $\nu_3 = 458 \text{ cm}^{-1}$ and $\nu_6 = 694 \text{ cm}^{-1}$ for the $^3\text{A}_1$ state at the CASSCF level. The frequencies $\nu_3 = 624 \text{ cm}^{-1}$ and $\nu_6 = 452 \text{ cm}^{-1}$ have been measured for the isoelectronic neutral FeCH_2 radical, in its ground electronic state, in an Ar matrix.^{30,31} While we do not rule out the possibility of transitions to two different electronic states, the similarities in widths of these peaks suggest transitions to a single state. Experiments with CoCD_2^+ would resolve many of these uncertainties.

NiCH₂⁺. The NiCH_2^+ photofragment spectrum, Figure 4, represents the first reported spectroscopic study of this molecule. In this system the parent signal level and photodissociation cross section are 1 order of magnitude lower than for FeCH_2^+ or CoCH_2^+ , degrading the signal/noise level as seen in the figure. Despite the low signal levels a threshold is observed at 406 nm, establishing $D^{\circ}_0(\text{Ni}^+-\text{CH}_2) \leq 295 \pm 5 \text{ kJ/mol}$. The very low signal level in this experiment increases the uncertainty in our value compared to those of FeCH_2^+ or CoCH_2^+ . This value is in slight disagreement with the ion-beam value measured by Fisher and Armentrout^{9,26} of $D^{\circ}_0(\text{Ni}^+-\text{CH}_2) = 306 \pm 4 \text{ kJ/mol}$, based on the endothermic $\text{Ni}^+ + \text{c-C}_3\text{H}_6$ and $\text{Ni}^+ + \text{c-C}_2\text{H}_4\text{O}$ reactions. For this system Bauschlicher et al.¹⁵ report $D^{\circ}_0(\text{Ni}^+-\text{CH}_2) = 322 \text{ kJ/mol}$, and Holthausen et al.²¹ $D^{\circ}_0(\text{Ni}^+-\text{CH}_2) = 307 \text{ kJ/mol}$. In contrast to FeCH_2^+ and CoCH_2^+ , for which the ground electronic state is one of a very nearly

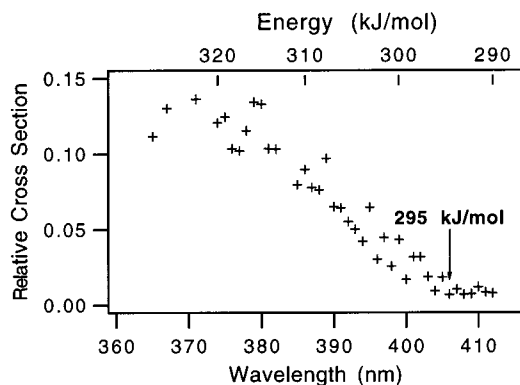


Figure 4. Photofragment spectrum of $\text{NiCH}_2^+ + h\nu \rightarrow \text{Ni}^+ + \text{CH}_2$. The Ni^+ photosignal is shown relative to that of Fe^+ from FeCH_2^+ , for which a value of 1 corresponds to approximately $4 \times 10^{-18} \text{ cm}^2$.

TABLE 1: Comparison of Spectroscopic Thresholds with Thermodynamic Bond Strengths for MCH_2^+ ($\text{M} = \text{Fe}, \text{Co},$ and Ni)

	spectroscopic threshold, ^a kJ/mol	thermodynamic bond strength, ^b kJ/mol
FeCH_2^+	342 ± 2	341 ± 4
CoCH_2^+	331 ± 2	318 ± 5
NiCH_2^+	295 ± 5	306 ± 4

^a This work. ^b As measured in the guided ion-beam experiments of Armentrout and co-workers.⁹

degenerate pair of states, the ground state of NiCH_2^+ is a single 2A_1 state.^{15,21}

Discussion

Spectroscopic vs Thermodynamic Thresholds. As presented in the previous section, the photodissociation spectra of internally cold MCH_2^+ ($\text{M} = \text{Fe}, \text{Co}, \text{Ni}$) have been obtained. For each system a spectroscopic threshold is observed. From these thresholds strict *upper limits* for the M^+-CH_2 bond strength may be set. In Table 1 we compare our *upper limit* values for $D^{\circ}_0(\text{M}^+-\text{CH}_2)$ with the thermodynamic bond strengths as measured in the guided ion-beam experiments of Armentrout and co-workers.⁹ In general the spectroscopic threshold will correspond to the thermodynamic bond strength if the molecule absorbs light *and* dissociates at threshold. Unsaturated transition metal-containing compounds do absorb widely. This prompted Freiser and co-workers, who performed much of the early work in this field, to suggest that the spectroscopic thresholds could be interpreted as thermodynamic thresholds; see for example ref 7. More recent, more precise measurements point to a more complicated picture. In a series of papers on diatomic molecules containing transition metals^{32–35} Morse, Armentrout, and co-workers have outlined the criteria for the observation of sharp dissociation thresholds and for interpreting these thresholds as the thermodynamic bond strengths. These criteria are that the molecule must have a large density of electronic states near the ground separated atom limit, and this separated atom limit must generate repulsive potential curves. Additionally, dissociation must be able to occur to the ground separated atom limit while preserving good quantum numbers, and there must be an absence of Franck–Condon difficulties in either the excitation or predissociation step. In other words the molecule cannot have regions above threshold in which its absorbance drops markedly or from which predissociation cannot occur. For example Co_2^+ , which has a sharp spectroscopic threshold at the thermodynamic bond strength, has 3458 electronic curves (Hund’s case c) arising from states within $10\,000 \text{ cm}^{-1}$ of the ground state separated

atom limit.³⁵ In this case the extremely high density of states is thought to preclude the need for repulsive curves. In contrast, neutral AlNi has 123 such electronic curves,³⁵ far fewer than Co_2^+ . That this molecule displays a sharp spectroscopic threshold is attributed to repulsive curves evolving from the $\text{Al}(s^2p^1, ^2P) + \text{Ni}(s^1d^9, ^3D)$ limit.³⁵ A third example involves Cr_2^+ . This molecule differs from both Co_2^+ and AlNi in that it does not exhibit a sharp dissociation threshold. Instead, Brucat and co-workers observe a much more gradual onset, complicated by vibrational structure.³⁶ Additionally, the spectroscopic threshold lies some 80 kJ/mol above the thermodynamic threshold as measured in an ion-beam experiment.³⁷ However, the first optically allowed transition for Cr_2^+ occurs to a state correlating to *excited* products which lie 90 kJ/mol above the ground separated atom limit.³⁵ If 90 kJ/mol is subtracted from the photodissociation threshold, there is reasonable agreement with the ion-beam value. Moreover, although Cr_2^+ has 222 electronic curves³⁵ arising from states within $10\,000 \text{ cm}^{-1}$ of the ground state separated atom limit, Morse, Armentrout, and co-workers³⁵ suggest that Franck–Condon difficulties give rise to a structured spectrum and prevent the molecule from exhibiting a sharp dissociation threshold. Previously⁵ we have measured the photofragment spectrum of FeO^+ (351 electronic curves within $10\,000 \text{ cm}^{-1}$). In this case only vibrationally resolved peaks are seen and the $0 \leftarrow 0$ transition occurs 8 kJ/mol above the thermodynamic threshold.

We may now use the criteria outlined by Morse, Armentrout, and co-workers³⁵ to aid in the interpretation of our results. As summarized in Table 1, our spectroscopic threshold for FeCH_2^+ is in exact agreement with the thermodynamic threshold. However, rather than observing a sharp spectroscopic threshold, we see a relatively gradual onset. The first of the criteria needing to be satisfied if a sharp spectroscopic threshold is to occur concerns the number of electronic states near the dissociation limit. Fe^+ has two low-lying excited states above the $^6D(3d^6 4s)$ ground state:²⁷ a $^4F(3d^7)$ state at 1872 cm^{-1} and a $^4D(3d^6 4s)$ state at 7955 cm^{-1} . The excited 1A_1 state of CH_2 lies 3147 cm^{-1} above the 3B_1 ground state.²⁸ The resulting molecule, FeCH_2^+ , has C_{2v} symmetry and thus does not have first-order spin–orbit splitting.²⁹ Therefore, the appropriate coupling case to employ when calculating the number of electronic states of FeCH_2^+ that correlate to $\text{Fe}^+ + \text{CH}_2$ is Hund’s case b. In this regime the states given above combine to give 63 curves arising from states within $10\,000 \text{ cm}^{-1}$ of the ground separated limit. It is immediately apparent that this is far fewer than the 3458 previously given for Co_2^+ . One reason for this drastic reduction stems from the different coupling schemes used to obtain these numbers. For the metal diatomics Hund’s case c coupling was employed,³⁵ causing each component of a spin–orbit multiplet to be counted as an individual electronic state. Under case b coupling the number of electronic states does not reflect spin–orbit states. If case c coupling were followed, 146 states would be predicted for FeCH_2^+ , still far fewer than for Co_2^+ . The overriding reasons for the low number of states are more physical in nature: first, CH_2 simply has far fewer low-lying electronic states than a typical transition metal, and second, the number of possible states is limited by the constraint of C_{2v} symmetry. The other criteria outlined by Morse, Armentrout, and co-workers³⁵ focus on whether the molecule can dissociate to ground-state fragments while preserving good quantum numbers and without Franck–Condon difficulties. As a result of the large increase in the symmetry around the metal upon dissociation, and because the ground state separated species are both open shell, optical transitions to states which correlate to

the ground state separated limit are allowed. Thus, the gradual onset of photodissociation is likely due to limited absorption to the few electronic states near the dissociation limit.

In contrast, CoCH_2^+ gives a sharper threshold than that for FeCH_2^+ . However, the upper limit value derived from this threshold, while a true upper limit, is 13 kJ/mol higher than the thermodynamic value.^{9,26} A second threshold lies 38 kJ/mol above the first. CoCH_2^+ has 77 electronic states (case b) arising from states within 10 000 cm^{-1} of the ground state separated atom limit, slightly more than FeCH_2^+ , which may explain the sharper thresholds. Again, transitions to states which correlate to ground state products are optically allowed. For this system however we do see evidence of a Franck–Condon progression, particularly above the second threshold. A structured spectrum would in general lead to an offset in the photodissociation threshold. The first excited states of Co^+ ($^5\text{F}_0$, $3d^7 4s$) and CH_2 ($^1\text{A}_1$) lie 40 and 38 kJ/mol above their respective ground states.^{27,28} Initially one might suspect that the second threshold arises once sufficient energy is present to allow dissociation to one of these excited states. However this second threshold lies 38 kJ/mol above the first threshold and *not* 38 kJ/mol above the ground state thermodynamic bond strength as measured by Armentrout and co-workers.^{9,26} We therefore conclude that this second threshold occurs once sufficient energy is available to access repulsive states of CoCH_2^+ arising from the ^5F or $^1\text{A}_1$ fragment states. While the difference in kinetic energy associated with release of ground versus excited-state fragments should in principle manifest itself in the widths of the fragment peaks at a given wavelength,³⁸ thus allowing us to differentiate between these two processes, 40 kJ/mol is an insufficient energy separation to enable us to do this for $\text{CoCH}_2^+ \rightarrow \text{Co}^+ + \text{CH}_2$.

We are in slight disagreement with the ion-beam measurement^{9,26} for NiCH_2^+ , since our spectroscopic onset gives an upper limit of $D^0_0(\text{Ni}^+-\text{CH}_2) \leq 295 \pm 5$ kJ/mol which is below the ion-beam value of $D^0_0(\text{Ni}^+-\text{CH}_2) = 306 \pm 4$ kJ/mol. However, due to a combination of poor parent signal levels, an unfavorable isotope distribution, and a low dissociation cross section, this measurement was made at our current detection limit. The low cross section likely arises because NiCH_2^+ has by far the fewest low-lying electronic states of the molecules reported here: only 36 states arise from states within 10 000 cm^{-1} of the ground state separated atom limit. The first excited state²⁷ of Ni^+ ($^4\text{F}_0$, $3d^8 4s$) is at 8394 cm^{-1} , a much larger separation from the ground state than in either Fe^+ or Co^+ .

Summary

Photofragment spectra of jet-cooled MCH_2^+ ($\text{M} = \text{Fe}, \text{Co}, \text{Ni}$) have been measured. The investigation of NiCH_2^+ represents the first reported spectroscopic study of this molecule. Spectroscopic thresholds are observed for each of the three systems which impose strict *upper limits* on the M^+-CH_2 bond strengths. Our results, in agreement with the ion-beam experiments of Armentrout and co-workers, show the bond strengths of these MCH_2^+ molecules to decrease along the period, $\text{M} = \text{Fe} > \text{Co} > \text{Ni}$. The measured upper limits are the following: $D^0_0(\text{Fe}^+-\text{CH}_2) \leq 342 \pm 2$ kJ/mol; $D^0_0(\text{Co}^+-\text{CH}_2) \leq 331 \pm 2$ kJ/mol; $D^0_0(\text{Ni}^+-\text{CH}_2) \leq 295 \pm 5$ kJ/mol. Three distinct, 2-nm-wide peaks are observed in the photofragment spectrum of CoCH_2^+ , but the spectra lack sharp structure above threshold. Criteria outlined by Morse, Armentrout, and co-workers for the interpretation of spectroscopic thresholds as thermodynamic

thresholds for diatomic molecules have been applied to the polyatomic MCH_2^+ systems.

Acknowledgment. Support of this work by a National Science Foundation Faculty Early Career Development Award (NSF CHE 9875220) is gratefully acknowledged.

References and Notes

- (1) Burwell, R. L., Jr. In *Heterogeneous Catalysis. Selected American Histories*; Davis, B. H., Hettinger, W. P., Jr., Eds.; ACS Symposium Series 222; American Chemical Society: Washington, DC, 1983; pp 3–12.
- (2) Eller, K.; Schwarz, H. *Chem. Rev.* **1991**, *91*, 1121.
- (3) Irikura, K. K.; Beauchamp, J. L. *J. Phys. Chem.* **1991**, *95*, 8344.
- (4) Anderson, R. B.; Kölbl, H.; Ralek, M. *The Fischer–Tropsch Synthesis*; Academic Press: Orlando, FL, 1984.
- (5) Husband, J.; Aguirre, F.; Ferguson, P.; Metz, R. B. *J. Chem. Phys.* **1999**, *111*, 1433.
- (6) Wiley, W. C.; McLaren, I. H. *Rev. Sci. Instrum.* **1955**, *26*, 1150.
- (7) Hettich, R. L.; Freiser, B. S. *J. Am. Chem. Soc.* **1986**, *108*, 2537.
- (8) Schultz, R. H.; Armentrout, P. B. *Organometallics* **1992**, *11*, 828.
- (9) Armentrout, P. B.; Kickel, B. L. In *Organometallic Ion Chemistry*; Freiser, B. S., Ed.; Kluwer Academic Publishers: Dordrecht, The Netherlands, 1994; pp 1–45.
- (10) McKee, M. L. *J. Am. Chem. Soc.* **1990**, *112*, 2601.
- (11) Veldkamp, A.; Frenking, G. *J. Chem. Soc., Chem. Commun.* **1992**, *2*, 118.
- (12) Veldkamp, A.; Frenking, G. *J. Comput. Chem.* **1992**, *13*, 1184.
- (13) Bauschlicher, C. W., Jr.; Langhoff, S. R. *Int. Rev. Phys. Chem.* **1990**, *9*, 149.
- (14) Bauschlicher, C. W., Jr.; Partridge, H.; Scuseria, G. E. *J. Chem. Phys.* **1992**, *97*, 7471.
- (15) Bauschlicher, C. W., Jr.; Partridge, H.; Sheehy, J. A.; Langhoff, S. R.; Rosi, M. J. *J. Phys. Chem.* **1992**, *96*, 6969.
- (16) Musaev, D. G.; Morokuma, K. *Isr. J. Chem.* **1993**, *33*, 307.
- (17) Musaev, D. G.; Morokuma, K.; Nobuaki, K. *J. Chem. Phys.* **1993**, *99*, 7859.
- (18) Musaev, D. G.; Morokuma, K.; Nobuaki, K.; Nguyen, K. A.; Gordon, M. S.; Cundari, T. R. *J. Phys. Chem.* **1993**, *97*, 11435.
- (19) Musaev, D. G.; Morokuma, K. *J. Chem. Phys.* **1994**, *101*, 10697.
- (20) Heinemann, C.; Hertwig, R. H.; Wesendrup, R.; Koch, W.; Schwarz, H. *J. Am. Chem. Soc.* **1995**, *117*, 495.
- (21) Holthausen, M. C.; Matthias, M.; Koch, W. *Chem. Phys. Lett.* **1995**, *240*, 245. The calculated D_e value has been converted to a D_0 value by applying a uniform 2 kJ/mol zero-point correction as suggested by the authors.
- (22) Ricca, A.; Bauschlicher, C. W., Jr. *Chem. Phys. Lett.* **1995**, *245*, 150.
- (23) Blomberg, M. R. A.; Siegbahn, P. E. M.; Svensson, M. *J. Chem. Phys.* **1996**, *104*, 9546.
- (24) Abashkin, Y. G.; Burt, S. K.; Russo, N. *J. Phys. Chem.* **1997**, *101*, 8085.
- (25) Armentrout, P. B.; Beauchamp, J. L. *J. Chem. Phys.* **1981**, *74*, 2819.
- (26) Fisher, E. R.; Armentrout, P. B. *J. Phys. Chem.* **1990**, *94*, 1674.
- (27) Moore, C. E. *Atomic Energy Levels, Circular 467*; National Bureau of Standards: Washington, DC, 1949.
- (28) Jensen, P.; Bunker, P. R. *J. Chem. Phys.* **1988**, *89*, 1327.
- (29) Herzberg, G. *Molecular Spectra and Molecular Structure, Vol. III: Electronic Spectra and Electronic Structure of Polyatomic Molecules*; Van Nostrand Reinhold Co.: New York, 1966.
- (30) Chang, S. C.; Kafafi, Z. H.; Hauge, R. H.; Billups, W. E.; Margrave, J. L. *J. Am. Chem. Soc.* **1985**, *107*, 1447.
- (31) Chang, S. C.; Hauge, R. H.; Kafafi, Z. H.; Margrave, J. L.; Billups, W. E. *J. Am. Chem. Soc.* **1988**, *110*, 7975.
- (32) Spain, E. M.; Morse, M. D. *Int. J. Mass Spectrom. Ion Processes* **1990**, *102*, 183.
- (33) Spain, E. M.; Morse, M. D. *J. Phys. Chem.* **1991**, *96*, 2479.
- (34) Russon, L. M.; Heidecke, S. A.; Birke, M. K.; Conceicao, J.; Armentrout, P. B.; Morse, M. D. *Chem. Phys. Lett.* **1993**, *204*, 235.
- (35) Russon, L. M.; Heidecke, S. A.; Birke, M. K.; Conceicao, J.; Morse, M. D.; Armentrout, P. B. *J. Chem. Phys.* **1994**, *100*, 4747.
- (36) Lessen, D. E.; Asher, R. L.; Brucat, P. J. *Chem. Phys. Lett.* **1991**, *182*, 412.
- (37) Su, C.-X.; Hales, D. A.; Armentrout, P. B. *Chem. Phys. Lett.* **1993**, *201*, 199.
- (38) Ding, L. N.; Kleiber, P. D.; Young, M. A.; Stwalley, W. C.; Lyyra, A. M. *Phys. Rev. A* **1993**, *48*, 2024.